Electrogenic K^+ Transport by the Kdp-ATPase of *Escherichia coli*†

Klaus Fendler,*,‡ Stefan Dröse,§ Karlheinz Altendorf,§ and Ernst Bamberg‡

Max-Planck-Institut für Biophysik, Kennedyallee 70, D-60596 Frankfurt/M, Germany, and Universität Osnabrück, Fachbereich Biologie/Chemie, Postfach 4469, D-49069 Osnabrück, Germany

Received January 24, 1996; Revised Manuscript Received April 4, 1996⊗

ABSTRACT: Charge translocation by the Kdp-ATPase of *Escherichia coli* was measured by adsorption of proteoliposomes to a planar lipid membrane. The proteoliposomes were prepared by reconstitution of purified Kdp-ATPase into liposomes prepared from *E. coli* lipids. The protein was activated by a ATP concentration jump produced by photolysis of a protected derivative of ATP, caged ATP. Charge translocation was measured with a time resolution of 15−40 ms. Stationary currents demonstrated the continuous pumping activity of the enzyme. Control measurements with the potential-sensitive dye $DiSC_3(5)$ showed a negative potential inside the proteoliposomes after activation with ATP. The measured electrical signals as well as the dye measurements correspond to the transport of positive charge to the intracellular face of the protein. The electrical signal was increased when K^+ was inside the proteoliposomes ($K_{0.5} \approx 50$ μM) and was inhibited by vanadate. These experiments demonstrate the electrogeneity of the Kdp-ATPase in a purified reconstituted system.

The Kdp system is a bacterial P-type ATPase of *Escherichia coli* that transports K^+ with high affinity [reviewed in Altendorf et al. (1992) and Altendorf and Epstein (1993)]. The transport complex consists of the membrane-bound subunits KdpA (59 kDa), KdpB (72 kDa), and KdpC (20 kDa). Recently, it was shown that a hydrophobic polypeptide with a molecular mass of 3 kDa, which is encoded by the open reading frame *kdpF* upstream of the first structural gene *kdpA*, is part of the transport complex (Möllenkamp and Altendorf, unpublished results). Since other members of the P-type ATPases consist of one or two subunits, it was suggested that the division of labor to three or four subunits is a presupposition to transport K^+ with high affinity (K_m = 2 μM) and high selectivity (Siebers & Altendorf, 1992). KdpB is the catalytic subunit and shares with other P-type ATPases 10 homologous regions identified by Serrano (1988). This polypeptide is the site of phosphorylation (Siebers & Altendorf, 1989), probably at the conserved residue Asp307 (Puppe et al., 1992), thereby providing the energy for K^+ transport by hydrolysis of ATP. KdpA is responsible for K^+ binding and transport. Evidence that KdpA has two binding sites for K^+ is based on the analysis of K_m mutants (Buurman et al., 1995). The function of KdpC is still subject to debate. Mutations in the *kdpC* gene render the complex defective in both K^+ transport and ATPase activity (Siebers & Altendorf, 1992). The *kdpFABC* operon is under control of the regulatory proteins KdpD and KdpE, which belong to the class of sensor kinase/response regulator systems (Walderhaugh et al., 1992). KdpD and KdpE mediate the expression of the structural genes only in media of low K^+ concentrations [reviewed in Altendorf et al. (1994)]. Therefore, the Kdp system can be characterized as an optional system to scavange K^+.

Although the Kdp system has been the subject of intensive genetic, physiological, and biochemical studies, little is known about the transport properties of the Kdp-ATPase. So far, the investigation of K^+ transport catalyzed by the Kdp system was restricted to intact cells (Rhoads et al., 1976). Net K^+ uptake via the Kdp system leads to depolarization of the cell membrane, suggesting that the transport process is electrogenic (Bakker & Mangerich, 1981). Recently, K^+ transport was demonstrated in right-side-out vesicles, using an ATP-generating system inside the lumen of the vesicles (Kollmann & Altendorf, 1993). However, partial reactions of the transport process could not be examined with this method.

Prominent members of the group of P-type ATPases are Na^+K^+- and H^+K^+-ATPases of eukaryotic cells. Overall transport in the Na^+K^+-ATPase is electrogenic (DeWeer et al., 1988) while it is electroneutral in the H^+K^+-ATPase (Sachs et al., 1976). This has been explained by electrogenic Na^+ and electroneutral K^+ countertransport in the Na^+K^+-ATPase (Gadsby et al., 1989). In contrast, in the H^+K^+-ATPase, electrogenic H^+ and electrogenic K^+ countertransport cancel out (Stengelin et al., 1993). These findings have important consequences for the transport mechanism relevant for ion transport, e.g., for the number of fixed countercharges cotransported during transport of the cations.

It is tempting to compare K^+ transport by the Kdp-ATPase with K^+ transport by the Na^+K^+- and H^+K^+-ATPases. The question arises whether this reaction is electrogenic in the Kdp-ATPase. Also, it is not known whether a transport step analogous to Na^+ or H^+ transport in H^+K^+- and Na^+K^+-ATPases exists in the Kdp-ATPase. In order to address these questions, we have investigated the electrical properties of the Kdp-ATPase.

MATERIALS AND METHODS

Growth of the Bacteria, Protein Purification, and Preparation of the Proteoliposomes. The *E. coli* K12 strain

† This work was supported by the Deutsche Forschungsgemeinschaft (SFB 169 and SFB 171) and the Fonds der Chemischen Industrie. S.D. was the recipient of a fellowship of the Graduiertenförderung des Landes Niedersachsen.

* To whom correspondence should be addressed.
‡ Max-Planck-Institut für Biophysik.
§ Universität Osnabrück.

⊗ Abstract published in *Advance ACS Abstracts,* June 1, 1996.

S0006-2960(96)00175-4 CCC: $12.00

TKA1000 (Siebers & Altendorf, 1988) was transformed with the plasmid pSR4 (Puppe et al., 1992) using the $CaCl_2$ method described in Maniatis et al. (1982). The resulting transformants carry the *kdp* genes on the chromosome and on the plasmid under control of the *kdp* promoter. The cells were grown in K0 minimal medium and were induced twice with 50 μM KCl (Siebers & Altendorf, 1988).

Starting with 25 g of the cells, the Kdp-ATPase was purified as described by Siebers et al. (1992), following the two-column procedure. All solubilization and purification steps were performed at 4 °C. As an extension of the protocol, the detergent Aminoxid WS35 was replaced by decyl maltoside, following a protocol of Dr. J. Naprstek and Dr. W. Epstein (University of Chicago, personal communication). The Kdp fraction pool of the Fractogel TSK AF-Red column (about 20 mL) was dialyzed against 1000 mL of 15 mM HEPES−Tris, pH 7.5, 0.035% Aminoxid WS35 for 12 h with two changes of the dialysis buffer. The dialyzed preparation was diluted with twice the volume of the same buffer containing 1% decyl maltoside and was then applied to a DEAE-Sepharose CL-6B column (1.5 × 3.5 cm), equilibrated with 15 mM HEPES−Tris, pH 7.5, 0.2% decyl maltoside (basal buffer). The column was washed with 5 column volumes of basal buffer. Elution was performed with 30 mL of a linear gradient of 0−200 mM NaCl in basal buffer wit a flow rate of 40 mL/h. Fractions of 2.5 mL were collected and analyzed by SDS−PAGE. The main fractions with a specific, K^+-stimulated ATPase activity of 5 μmol·g^{-1}·min^{-1} were pooled and stored in liquid nitrogen.

For the preparation of proteoliposomes, 250 μL of purified Kdp-ATPase (0.78 mg/mL protein in 15 mM HEPES−Tris, pH 7.5, 100 mM NaCl, and 0.2% decyl maltoside) and 250 μL of *E. coli* lipid (10 mg/mL, 10 mg/mL $C_{12}E_8$, 85 mM Tris-HCl, pH 7.5, and 4 mM $MgSO_4$) were mixed and incubated on ice for 15 min. Then 500 μL of Bio-Beads SM-2 (Bio-Rad) was added and the solution stirred for 20 h at 6 °C. The Bio-Beads were replaced by fresh Bio-Beads, and the solution was stirred for 1 h at room temperature. The suspension was centrifuged at 7000*g* for 2 min, and the pellet containing the Bio-Beads was discarded. The proteoliposomes were sonnicated for 10 s before use. To determine the enzymatic activity of the Kdp-ATPase, proteoliposomes were centrifuged for 45 min at 225000*g*, and the pellet was resuspended in half of the starting volume in 15 mM HEPES−Tris, pH 7.5. The protein concentration was determined with the amido black method (Schaffner & Weissmann, 1973). The ATPase activity was analyzed by the method described in Siebers and Altendorf (1988).

Bilayer Measurements. Optically black lipid membranes (BLM) with an area of 0.01−0.02 cm^2 were formed in a thermostated Teflon cell as described elsewhere (Fendler et al., 1985; Borlinghaus et al., 1987). Each of the two compartments of the cell was filled with 1.5 mL of electrolyte containing 50 mM Tris-HCl, pH 7.5, 2 mM $MgSO_4$, 1 mM DTT, and various amounts of caged ATP and KCl. The temperature was kept at 24 °C. The membrane-forming solution contained 1.5% (w/v) diphytanoylphosphatidylcholine and 0.025% (w/v) octadecylamine dissolved in *n*-decane. The membrane was connected to an external measuring circuit via polyacrylamide gel salt bridges and Ag/AgCl electrodes. The signal was amplified, filtered (cutoff frequency = 500 Hz), and recorded with a digital oscilloscope, 50 μL of the proteoliposomes was added to one compartment of the cuvette and stirred for 30 min. Caged ATP and, if necessary, ionophores were added under stirring to the cuvette.

To photolyze the caged ATP, light pulses of an excimer laser (duration 10 ns, wavelength 308 nm) or of a high-pressure mercury arc lamp (duration 125 ms) were focused onto the lipid bilayer membrane. The intensity at the membrane surface was adjusted to a level that 15−30% of the caged ATP was photolyzed. After each flash, the system was kept in the dark and stirred for 10 min to allow dilution of the ATP released during the flash and its hydrolysis by the enzyme present in solution. The fraction of caged ATP converted to ATP at the membrane surface was determined in the cuvette in the absence of Kdp-ATPase with a luciferin−luciferase assay as described previously (Nagel et al., 1987).

The conductivity of the membrane was varied by addition of the protonophore 1799, the electroneutral proton/cation exchanger monensin, or the K^+-ionophore valinomycin in an ethanolic solution to both compartments. The conductivity was measured by applying a voltage of 10 mV to the membrane and measuring the induced current.

Caged ATP, P^3-[1-(2-nitrophenyl)ethyl]adenosine 5′-triphosphate, was prepared as described elsewhere (Fendler et al., 1985) and kindly provided by Dr. E. Grell, MPI für Biophysik, Frankfurt, FRG. Concanamycin A was a generous gift of Prof. Dr. A. Zeeck, Universität Göttingen, FRG, and the CIBA AG, Basel, CH.

Fluorometric Measurements. The fluorometric measurements were carried out in 1 mL of solution containing 50 mM Tris-HCl, pH 7.5, 2 mM $MgSO_4$, and 50 mM KCl together with 1 μM of the potential-sensitive fluorophore $DiSC_3(5)$ and 20 μL of the proteoliposomes. The settings of the fluorometer were as follows: excitation wavelength, 650 nm; emission wavelength, 675 nm; band-pass, in both cases 5 nm; integration time, 1 s.

RESULTS

Characterization of the Proteoliposomes. For a characterization of the proteoliposomes, the size distribution was determined by inelastic light scattering. A broad distribution of diameters ranging from 50 to 200 nm was found. The enzymatic activity of the proteoliposomes was determined as described under Materials and Methods. The protein determination revealed that 30% of the supplied Kdp-ATPase was incorporated into the proteoliposomes. The K^+-stimulated ATPase activity was found to be around 15 μmol·mg^{-1}·min^{-1}. Surprisingly, an identical enzymatic activity was determined in the presence and absence of the K^+ ionophore valinomycin. These results are difficult to reconcile in light of a strict coupling of hydrolysis and transport in these types of ion pumps. A possible explanation could be that different populations of the enzyme contribute to the measurement of hydrolysis and electrical activity, respectively. The same conclusions were drawn from the analysis of the effect of inhibitors and are discussed in more detail under Discussion.

From the amount of incorporated protein, we estimated the number of pumps per liposome using the following values: liposome diameter, 50−200 nm; membrane thickness, 4 nm; lipid density, 1 g·cm^{-3}; protein/lipid weight ratio, 2.4 × 10^{-2}; molecular mass of Kdp-ATPase, 154 kDa

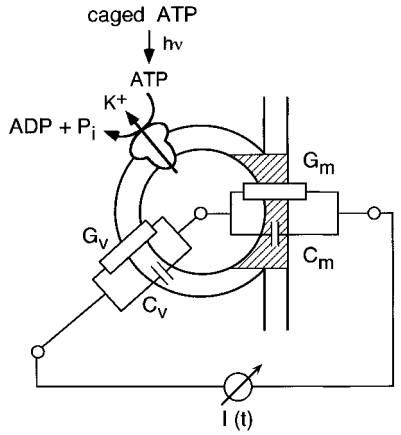

FIGURE 1: Compound membrane: proteoliposome adsorbed to the planar lipid membrane. The current generated by the integrated Kdp-ATPase is coupled to the measuring system [$I(t)$] via the conductivities G_m, G_v and capacitances C_m, C_v of the proteoliposome and the planar lipid membrane.

(assuming a monomeric functional unit); fraction of inside-out oriented pumps, 0.1. This yields 0.3 (50 nm) to 5 (200 nm) pumps per liposome. The value given in parentheses is the corresponding diameter of the liposome. Based on an activity of 15 μmol·mg^{-1}·min^{-1}, the turnover of the pumps at maximal ATP activation is 40 s^{-1}. Assuming one ion transported per cycle, we obtain an initial pumping rate of 0.08 (200 nm) to 0.4 mM·s^{-1} (50 nm) and an initial voltage increase of 20 mV/s. These values have to be compared with the passive permeability of liposomes for protons, which is approximately 10^{-4} cm·s^{-1} (Levy et al., 1990). A gradient of 1 pH unit (outside, pH 7.5; inside, pH 6.5) yields a proton flux of 0.01 (200 nm) to 0.04 mM·s^{-1} (50 nm). This is smaller than the pump currents. However, in the presence of Cl^-, a much higher proton permeability is to be expected (Levy et al., 1990), which may be in the range of the pump currents.

Finally, the activity of the incorporated enzyme can be compared to the measured currents. Under the conditions of the experiment, i.e., in the presence of caged ATP, the enzyme is only half-activated (turnover, 20 s^{-1}). Assuming complete coverage of the lipid membrane (diameter 1 mm) with liposomes of 100 nm diameter, we calculate a current of 300 pA. This is in reasonable agreement with values of 100−200 pA measured in the electrical experiments and supports the estimations made above.

Fluorometric Measurements. The fluorescence experiments were performed at high K^+ concentrations to minimize the effect of K^+ gradients created by the ion pump. ATP-driven K^+ depletion in the proteoliposomes results in a negative potential inside, which can be monitored with the dye $DiSC_3(5)$ (Hoffman & Laris, 1974). Before activation of the Kdp-ATPase, the K^+-concentration in and outside the proteoliposomes was 50 mM. After addition of 3 mM ATP, the fluorescence intensity decreases (Figure 2a), indicating the buildup of a negative potential inside the proteoliposomes. This demonstrates the expulsion of K^+ ions out of the proteoliposomes. Addition of the K^+ ionophore valinomycin allows the backflow of the expelled K^+ and, consequently, abolishes the potential as shown in Figure 2a. Inhibition by vanadate is demonstrated by the increase of fluorescence (Figure 2b). This shows that the liposomes are relatively permeant to ions, since the negative potential

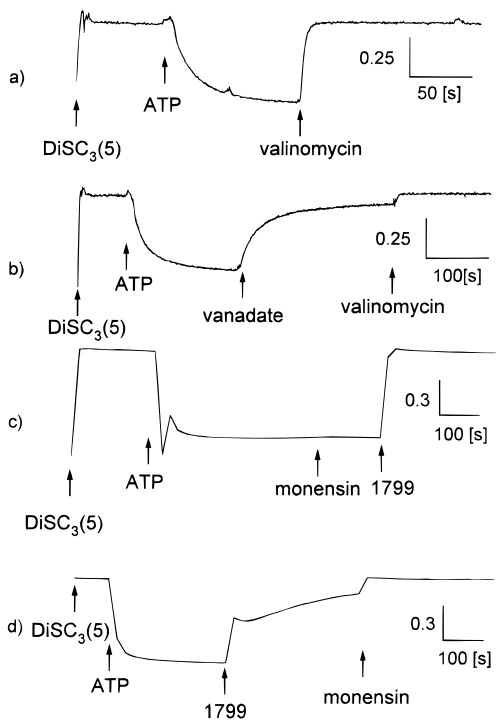

FIGURE 2: $DiSC_3(5)$ fluorescence measurement of proteoliposomes. Relative fluorescence changes are plotted in the figure. Addition of ATP and the ionophores is indicated. Buffer: 50 mM Tris-HCl, pH 7.5, 2 mM $MgSO_4$, 50 mM KCl, 1 μM $DiSC_3(5)$, and 20 μL of the proteoliposome-containing suspension. Additions: 3 mM ATP, 1 μM valinomycin, 10 μM monensin, 1 μM 1799, 1 mM orthovanadate.

relaxes after inhibition of the ion pump with a time constant of about 20 s. The negative potential inside the proteoliposomes is not affected by the electroneutral K^+/H^+-carrier monensin and decays only after the addition of the electrogenic carrier 1799 (Figure 2c). Addition of the protonophore 1799 alone leads to a partial and slow decay of the potential (Figure 2d), because inflowing protons can compensate for the charge of the extruded K^+ ions. The influx of protons, however, is hampered by the creation of a pH gradient across the proteoliposome membrane. Only after addition of monensin can the pH gradient be dissipated together with the K^+ gradient generated by the ion pump.

Characterization of the Electrical Signal. Electrical currents generated by the Kdp-ATPase were measured with a technique which has been previously applied to a number of other electrogenic ion pumps (Bamberg et al., 1991). Proteoliposomes were adsorbed to the BLM as described under Materials and Methods. The configurations of ion pumps, the proteoliposomes, and the supporting planar lipid membrane are illustrated in Figure 1. Using an inactive photolabile ATP derivative (caged ATP; Kaplan et al., 1978), an ATP concentration jump can be generated by illumination of the compound membrane with UV light. In the experiments described below, 10−30% of caged ATP is converted to ATP.

For the data shown in Figure 3, an UV lamp was used as light source. In all other experiments, caged ATP was photolyzed using an excimer laser flash. Using the UV lamp, ATP was released within the shutter opening time of 125 ms. Faster release of ATP can be obtained with an UV laser flash. There the release is limited by the time constant of the photolytic dark reaction which is about 44 ms at pH 7.5,

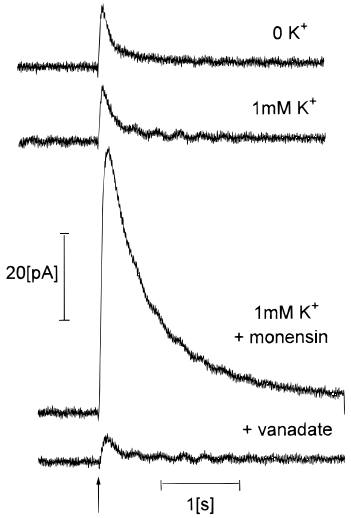

FIGURE 3: Electrical current measured after release of ATP by a UV light flash. Light source: Hg high-pressure lamp, flash duration 125 ms. Buffer: 50 mM Tris-HCl, pH 7.5, 2 mM $MgSO_4$, 1 mM DTT. Caged ATP concentration before the UV flash: 300 μM. Additions of 10 μM monensin, 1 mM orthovanadate, or 1 μM 1799 to the buffer are indicated at the corresponding traces.

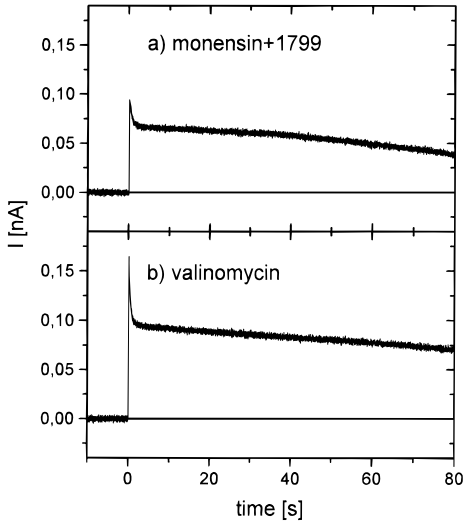

FIGURE 4: Stationary current after addition of ionophores. Light source: UV laser. Buffer: 50 mM Tris-HCl, pH 7.5, 2 mM $MgSO_4$, 1 mM KCl, 1 mM DTT. Caged ATP concentration before the UV flash: 300 μM. (a) 1 μM 1799 and 10 μM monensin, conductivity $G = 130$ nS/cm^2. (b) 1 μM valinomycin, conductivity $G = 240$ nS/cm^2.

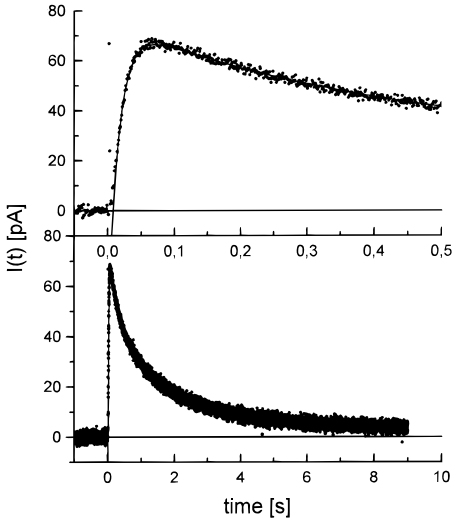

FIGURE 5: Time dependence of the electrical signal. Light source: UV laser. Buffer: 50 mM Tris-HCl, pH 7.5, 2 mM $MgSO_4$, 1 mM KCl, 1 mM DTT. Caged ATP concentration before the UV flash: 600 μM. The solid line is a fit to the data using eq 1. This is a high time-resolution plot of the data set shown in Figure 6 before addition of ionophores (33 nS/cm^2). The parameters of the fit are shown in Table 1.

2 mM Mg^{2+}, and 24 °C (Walker et al., 1988; Barabás & Keszthelyi, 1984).

Figure 3 shows the currents generated in the absence and presence of K^+ and the inhibitor vanadate. Also in the absence of K^+ a small electrical signal was obtained. Part of this signal is probably due to residual K^+ in the nominally K^+-free solution. After addition of 1 mM K^+, the signal did not increase until 10 μM monensin was added. The electroneutral K^+/H^+ exchanger monensin enabled K^+ to enter the proteoliposomes and to activate the ion pump, which resulted in a 4-fold increase of the peak current. This indicates that K^+ activates the pump *in vivo* at the extracellular side of the protein.

Addition of 1 mM orthovanadate inhibited the electrical signal. The origin of the small remaining peak is not clear. In an experiment with protein-free liposomes, such a signal was not observed, confirming that the residual signal is not a light artifact. Furthermore, under the same conditions, vanadate inhibits ATP hydrolysis completely. At subsequent flashes, the reduced signal remained constant while addition of vanadate up to 3 mM reduced the signal even further. Apparently, turnover of the enzyme is inhibited by vanadate with higher affinity than the electrical signal. Concanamycin A is an inhibitor of the Kdp-ATPase (Dröse et al., 1993). However, using up to 100 μM concanamycin, the electrical signal was not affected, whereas ATP hydrolysis is inhibited by 80%. For this unexpected behavior, a tentative explanation which envolves two different enzyme populations is given under Discussion.

By the addition of ionophores, the lipid membranes can be made conductive. This allows the measurement of a stationary current. Applying the protonophore 1799 together with the K^+/H^+ exchanger monensin, which together act as a H^+ and K^+ transport system, a stationary current over many seconds was observed (Figure 4). This demonstrates a continuous pumping activity of the Kdp-ATPase after activation with ATP. In a second experiment, the membrane was made conductive by addition of the K^+ ionophore valinomycin. Also under these conditions a stationary current of comparable magnitude was observed. Note that the conductivity in both cases was approximately the same. These two experiments demonstrate that the transport activity of the Kdp-ATPase is the same whether the membranes are conductive for K^+ and H^+ or for K^+ alone.

Time Dependence of the Transient Current. The light pulses of the UV laser have a duration of only 10 ns. The release of ATP is limited by the reactions in the caged compound following absorption of the photon. Therefore, under the conditions of the experiments, ATP is released after a laser flash with a time constant of about 44 ms (Walker et al., 1988; Barabás & Keszthelyi, 1984).

A time-resolved current trace after the release of ATP is shown in Figure 5. The current was analyzed by fitting a three-exponential function to the signal:

$$I(t) = A_1 e^{-t/\tau_1} + A_2 e^{-t/\tau_2} + A_3 e^{-t/\tau_3} + I_\infty \qquad (1)$$

with the time constants τ_1, τ_2, and τ_3 and the stationary current I_∞. In a typical electrical signal in the absence of ionophores (e.g., Figure 5), the current rises with a time constant of ca. 20 ms and decays with two time constants of ca. 0.5 s and 3 s. As will be shown in the following, the rise of the signal is dominated by the rate of release of ATP from caged ATP. The decay is attributed to the charging of the proteoliposomes and the buildup of ionic gradients following the pumping activity of the enzyme.

Variation of the Conductivity of the Compound Membrane. The ion pump is coupled to the measuring system via the conductivities and the capacitances of the proteoliposomes and the supporting planar lipid membrane (see Figure 1). In the following, proteoliposomes and supporting planar lipid membrane will be refered to as compound membrane. It is characterized by the system time constant $\tau_0 = (C_m + C_v)/(G_m + G_v)$ (Fendler et al., 1993). G_m and G_v are the conductivities of the planar bilayer and the proteoliposomes and C_m and C_v are their capacitances. This time constant describes the charging of the proteoliposomes after activation of the ion pump.

In Figure 6, the measured currents are shown at different conductivities of the membranes. In this experiment, the conductivity was varied by addition of the K^+ ionophore valinomycin. The conductivity of the poroteoliposomes/planar lipid membrane compound system was measured by applying a voltage of 10 mV to the membrane. The measured conductivity was used as an estimate for the conductivity of proteoliposomes and the planar lipid membrane. At low conductivities, the measured current decays to zero while at high cnductivities it rises to its maximum value without an overshoot (see Figure 6).

The signals shown in Figure 6 were analyzed with the fit function given in eq 1. The results of the fit are given in Table 1. The signal rises with a time constant of $\tau_1 \approx 20$ ms. At low conductivities, the signal decays with two time constants. The first time constant ($\tau_2 = 0.37$ s) of the decay is comparable to the sytem time constant found for Na^+K^+-ATPase containing membrane fragments ($\tau_0 = 100-200$ ms; Fendler et al., 1993) and proteoliposomes ($\tau_0 \approx 200$ ms; unpublished results) adsorbed to a planar lipid membrane.

This signal may be understood by assuming that the current generated by the Kdp-ATPase is approximately a step function and that τ_2 represents the system time constant τ_0. At $t \rightarrow 0$, the current is dominated by capacitive coupling and proportional to $C_v/(C_v + C_m)$ [see Figure 1 and Fendler et al. (1993)]. This is obvious from Figure 6 where the currents rise rapidly to a value which is independent of the conductivity of the compound membrane. Starting from this value, the current rises or decays with the time constant τ_2. τ_2 is relatively independent of the conductivity but, at high conductivities, decreases (Table 1) as expected for the system time constant $\tau_0 = (C_m + C_v)/(G_m + G_v)$. At $t \rightarrow \infty$, the current is proportional to the conductivities of the membranes, $G_v/(G_v + G_m)$, and rises with increasing conductivity as seen in the figure.

The arguments given above show that on a time scale relevant for the electrical properties of the compound membrane ($t > 100$ ms) the current generated by the pump can be approximated by a step function. The system time

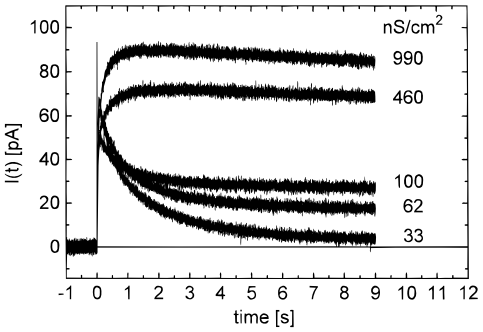

FIGURE 6: Electrical signal at different conductivities of the compound membrane. Light source: UV laser. Buffer: 50 mM Tris-HCl, pH 7.5, 2 mM $MgSO_4$, 1 mM DTT, 1 mM KCl. Caged ATP concentration before the UV flash: 600 μM. The conductivity was varied by addition of 1−10 μM valinomycin.

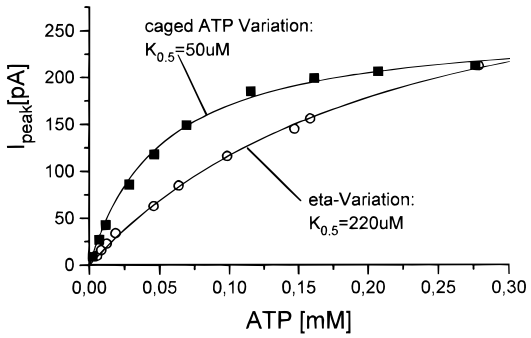

FIGURE 7: ATP dependence of the peak current. Light source: UV laser. (■) Variation of the ATP concentration by addition of caged ATP; fraction of released ATP, $\eta = 0.15$. (○) Variation of the ATP concentration by using different light intensities; caged ATP concentration before the UV flash, 600 μM.

Table 1: Time Constants from Fits to the Data Sets Shown in Figure 6

G (nS/cm²)	τ_1 (ms)	τ_2 (s)	τ_3 (s)
33	17	0.37	2.0
62	20	0.56	2.2
100	21	0.67	5.9
460	27	0.50	17
990	17	0.23	17

constant in the absence of ionophores is found to be about 500 ms. This value is in agreement with comparable measurements on membrane fragments ($\tau_0 = 100-200$ ms; Fendler et al., 1993) and proteoliposomes ($\tau_0 \approx 200$ ms; unpublished results) containing Na^+K^+-ATPase. The origin of the third time constant, $\tau_3 \approx 2$ s, is unclear and may be related to the buildup of concentration gradients during the activity of the pump.

ATP Dependence of the Transient Current. The amount of ATP released after a UV flash depends on the intensity of the light and the concentration of caged ATP present. Different light intensities yield different fractions, η, of released ATP. The ATP dependence can therefore be studied by variation of the amount of caged ATP present in solution or by variation of the intensity of the UV light. In Figure 7, the peak current is plotted at different concentrations of released ATP. The ATP concentration was increased by addition of increasing amounts of caged ATP (black squares). Subsequently, the UV light intensity was reduced, yielding decreasing ATP concentrations (open circles). The two traces do not superimpose, showing that the pumping activity

Table 2: Time Constants at Different Concentrations of Caged ATP

c_c^0 (μM)	τ_1 (ms)	τ_2 (s)	τ_3 (s)
30	44	2.7	
50	43	2.5	
120	37	1.4	
200	33	1.1	20
300	31	0.56	11
500	26	0.67	7.1
700	23	0.63	5.9
900	22	0.59	5.6
1200	19	0.53	4.8

of the enzyme depends on both the ATP and the caged ATP concentrations.

In our experiments, substrate and inhibitor are simultaneously present at concentrations of ηc_c^0 and $(1 - \eta)c_c^0$, respectively. Here c_c^0 is the concentration of caged ATP before the light flash. For competitive inhibition of the Kdp-ATPase by caged ATP, the enzyme activity is given by

$$v = v_{max}\frac{\eta c_c^0}{\eta c_c^0 + K_a\{1 + [(1 - \eta)c_c^0]/K_c\}} \qquad (2)$$

K_a and K_c are the dissociation constants for substrate and inhibitor binding, respectively. Equation 2 can be transformed to yield a hyperbolic dependence on ATP for the two cases of the experiment, η = constant and c_c^0 = constant, the apparent binding constants being

$$K'_a(\eta = \text{constant}) = \frac{\eta K_a K_c}{\eta K_c + (1 - \eta)K_a}$$
$$K'_a(c_c^0 = \text{constant}) = K_a\frac{K_c + c_c^0}{K_c - K_a} \qquad (3)$$

From a fit with a hyperbolic ATP concentration dependence to the data of Figure 7, apparent binding constants were determined in both cases, and the ATP and caged ATP binding constants were calculated using eq 3. For ATP, a binding constant of $K_a = 70$ μM and for caged ATP an inhibition constant of $K_c = 630$ μM were found.

The ATP binding constant found in the electrical experiments is comparable to that found for ATP hydrolysis ($K_m = 80$ μM; Siebers & Altendorf, 1988). The electrical experiments clearly indicate an inhibitory effect of caged ATP, probably a competitive inhibition. A 10 times weaker binding of caged ATP compared to ATP was found which is comparable to the situation in Na^+K^+-ATPase (Nagel et al., 1987). However, it is worth mentioning that the enzymatic activity of the solubilized Kdp-ATPase is not affected by caged ATP. This is in clear contradiction to the electrical experiments. At present, we have no explanation for this surprising finding.

In addition to the peak current, also the time constants of the electrical signal change at different concentrations of caged ATP. This is shown in Table 2. At low caged ATP concentrations, only two exponential functions were required to describe the signal. With increasing caged ATP concentration, the signal rises more rapidly and decays faster.

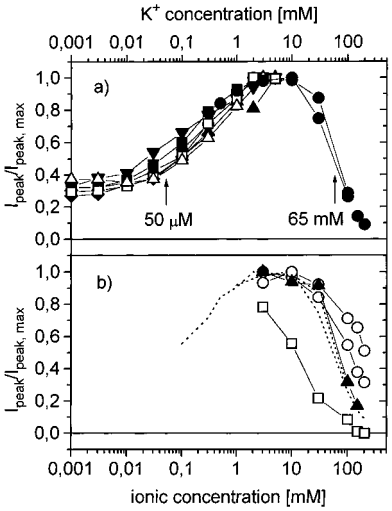

FIGURE 8: Dependence of the normalized peak current on the concentration of various cations and anions. Light source: UV laser. Caged ATP concentration before the UV flash: 300 μM. Buffer as in Figure 3. (a) K^+ dependence in the presence of (■) 0.1 μM valinomycin; (□) 1 μM valinomycin 1.1 μM 1799; (◆) 0.1 μM valinomycin, 0.1 μM 1799; (△) 0.1 μM valinomycin, 0.1 μM 1799; (▲) 0.1 μM valinomycin; (▼) 10 μM monensin; (●) 10 μM monensin, 1 μM 1799. (b) Dependence on various salts in the presence of 1 mM KCl. (○) Cholinechloride dependence; (▲) NaCl dependence; (□) $NaClO_4$ dependence. For comparison, a KCl dependence of part a is included (dotted line). Note that some of the dependencies were recorded in duplicate.

At low caged ATP concentration, the signal rises with a time constant of approximately 40 ms, which agrees with the time constant of release of ATP from caged ATP (44 ms; Walker et al., 1988; Barabás & Keszthelyi, 1984). The fact that values for $\tau_1 < 40$ ms are obtained at large concentrations can be explained by the high ATP concentration released. Under these conditions, the ATP binding site is saturated before all of the ATP is released, and a shorter risetime of the signal is measured. The conductivity dependence suggests that the decay of the signal with $\tau_2 \approx 0.5$ s is due to the system time constant τ_0 of the compound membrane. Its increase at low caged ATP concentrations (up to 2.7 s) is possibly due to a slow process which under these conditions dominates the decay of the signal.

Dependence of the Transient Current on Different Cations and Anions. The K^+ dependence of the transient currents is shown in Figure 8a, where six different experiments are summarized. For comparison of the different experiments, the peak currents I_{peak} shown in the figure are normalized to their maximal value $I_{peak,max}$. As shown with different ionophores (see figure legend), the accessibility of the internal volume of the proteoliposomes or the buildup of an electrochemical potential does not influence the measurements. Already at nominally zero K^+ concentration, a current could be measured. This may be attributed to the high K^+ affinity of the enzyme ($K_{0.5} = 2-10$ μM; Rhoads et al., 1976; Siebers & Altendorf, 1988) and the residual amount of K^+ in a nominally K^+-free buffer. From the figure, a half-saturation concentration for the activation of the enzyme with K^+ of about 50 μM can be estimated.

At high K^+ concentrations (about 65 mM), the current generated by the Kdp-ATPase is reduced. This was analyzed in more detail by addition of different cations and anions to a solution which already contained 1 mM KCl. As shown in Figure 8b, the addition of NaCl, cholinechloride, or

$NaClO_4$ reduces the signal. However, the effect of the different cations and anions is significantly different: NaCl performs like KCl; cholinechloride is less and $NaClO_4$ is much more effective than KCl. This demonstrates that the reduction of the signal at high salt concentration is not an inhibitory effect of K^+ at its release site nor is it a simple ionic strength effect.

DISCUSSION

P-Type ATPase catalyze the transport of a variety of cations such as H^+, Na^+, K^+, and Ca^{2+}. In many cases, two different ion types are transported sequentially in opposite directions. Countertransport can be energetically favorable, because it reduces the transported net charge. If the pump has to work against extreme ion concentrations, electroneutral operation is the preferred principle of design. This is realized in the H^+K^+-ATPase from parietal cells of the stomach, where two H^+ ions are exchanged against two K^+ ions (Rabon et al., 1982). Electrogenic transport can contribute or act against the membrane potential. In turn, the pump activity may be regulated by the membrane potential. Determination of the electrogeneity of transport is therefore important for the energetics of the pump, for its regulation, and for cell function.

Kdp-ATPase Is Electrogenic. Electrogeneity of the Kdp-ATPase has been investigated on whole cells (Bakker & Mangerich, 1981). Net K^+ uptake leads to depolarization of the cell membrane. However, in native membranes, electrogeneity of a single component is difficult to determine, since other membrane proteins may contribute to charge translocation. Therefore, in this paper we used purified Kdp-ATPase reconstituted into liposomes. In the fluorescence measurements (Figure 2), it was shown that the purified Kdp-ATPase reconstituted into liposomes generates a negative potential inside when activated by ATP. These measurements demonstrate that during the Kdp reaction cycle a positive charge is transported to the cytoplasmic side of the protein. Direct evidence for that stems from electrical measurements. According to our experimental configuration, a positive current represents a translocation of positive charge toward the lipid bilayer. Only enzyme molecules reconstituted in the liposomes with their intracellular side facing outward can be activated by ATP generated in the buffer. Consequently, the electrical measurements show that upon activation with ATP positive charge is transported to the cytoplasmic side of the protein. Therefore, both the fluorescence as well as the electrical measurements demonstrate the electrogenic nature of ion transport by the Kdp-ATPase.

Both inhibitors, vanadate and concanamycin, seem to be more effective under turnover conditions than in the electrical experiments. A similar effect is found for valinomycin, which stimulates the electrical signal in the same way as monensin does (Figure 3) while being inefficient in activating hydrolysis of ATP by the proteoliposomes (see Results). Two alternative explanations can account for this behavior: (1) The reaction steps contributing to the electrical signal are different from those that determine hydrolysis, namely, the rate-limiting step. (2) Different populations of the reconstituted enzyme are responsible for the different measurements. Hypothesis 1 has to be rejected because the electrical signal represents the stationary state of the Kdp-ATPase (see below). Hypothesis 2 can account for the behavior observed in our experiments in the following way: The majority of ion pumps are "unoriented". This means an association with the liposome which leaves the ATP binding sites accessible from the outside but transport across the membrane does not occur. "Unoriented" ATPases are not unusual for liposome preparation. Up to 70% of unoriented Na^+K^+-ATPase have been reported for Na^+K-ATPase proteoliposome preparations (Cornelius, 1988; Hilden & Hokin, 1975). This population is sensitive to inhibitors but cannot be activated by valinomycin. By its large number, these enzymes dominate hydrolysis. In contrast, the electrical signal is generated by an "oriented" population which is not sensitive to inhibitors. These pumps determine the results obtained by the electrical experiments while the "unoriented" population is electrically silent.

H^+ Countertransport? The Kdp-ATPase is a P-type ATPase like the mammalian Na^+K^+-ATPase which has been intensively investigated in the past. Comparison of the transport mechanism of the Na^+K^+-ATPase with the Kdp-ATPase may provide valuable insight into the transport mechanism of the Kdp-ATPase. The Na^+K^+-ATPase transports three Na^+ ions to the extracellular medium and imports two K^+ ions into the cell. Na^+ transport is associated with the formation of the phosphointermediate E_2P while K^+ transport takes place after dephosphorylation of the enzyme, probably during the $E_2 \rightarrow E_1$ transition [for a review, see Läuger (1991)]. Since the Kdp-ATPase transports K^+ into the cell, it seems reasonable to assign the K^+ transport events in Kdp- and Na^+K^+-ATPase to the same reaction steps, namely, the $E_2 \rightarrow E_1$ transition. The question now arises whether there is a transport event in Kdp-ATPase which is analogous to Na^+ transport and formation of E_2P. Since H^+ countertransport is a possible candidate for this reaction, the following, tentative reaction mechanism for the Kdp-ATPase could be envisaged: extrusion of one H^+ out of the cell followed by the import of two K^+ into the cell. The transport of two K^+ ions was chosen in analogy to the Na^+K^+-ATPase. Since we found positive charge transported to the intracellular side of the protein, the transport of zero and one H^+ are both consistent with the experimental data obtained.

Under the conditions used in the fluorescence experiments, the pump is most probably controlled by the generated potential rather than by ion gradients (see Results). This makes assessment of H^+ transport difficult. In addition, the high passive permeability for protons of the liposomes complicates the interpretation of the experiments. Therefore, the fluorescence measurements, while showing no indication for H^+ transport, do not rule out H^+ countertransport.

Also, the electrical experiments are consistent with the notion that the Kdp-ATPase transports exclusively K^+ ions because a stationary current is obtained when the membrane is permeable only for K^+ ions. An additional conductivity for H^+ does not significantly change the stationary current (see Figure 4). Under the conditions used in the experiment, the buffer has a relatively low buffer capacity of ca. 6 mM. In the time range of the experiment (100 s), the pump transports approximately 8−40 mM ions. This seems to exceed the buffer capacity leading to a strong acidification of the liposome interior. However, in view of the considerable proton permeability of the liposomes, a definite conclusion about H^+ countertransport is difficult.

In summary, we have found no indication that in the Kdp-ATPase H^+ countertransport takes place. However, based

on our experiments, we cannot rigorously exclude this possibility. If we adopt a model analogous to the Na^+K^+-ATPase, the formation of the phosphoenzyme in the Kdp-ATPase corresponds either to the transport of one H^+ ion out of the cell or to the return of the unloaded K^+ binding sites to the extracellular surface.

The Electrical Signal. The measured time-resolved current potentially contains information about partial reactions during the enzymatic activity of the enzyme. However, in addition to the properties of the enzyme, also the principle of the measurement itself influences the signal. As has been shown previously, the system time constant τ_0 and the time of photolytic release of the substrate are contained in the signal (Fendler et al., 1993). These processes have to be identified in the electrical signal if kinetic information about the ion pump is to be extracted.

The electrical signal rises with a time constant of $\tau_1 \approx 15-50$ ms. τ_1 is independent of the conductivity of the membrane (Table 1) and has to be assigned to the time constant of the release of ATP from caged ATP (44 ms under the conditions of the experiment).

The system time constant τ_0 describes the discharge of the compound membrane after charging by the electrogenic activity of the ion pump. As mentioned under Results, the time constant $\tau_2 \approx 0.5$ s (at saturating caged ATP concentrations) was assigned to the system time constant τ_0.

The third time constant, $\tau_3 = 2-17$ s, is much too large to be part of the reaction cycle of the Kdp-ATPase. It disappears at low activation of the ion pump (Table 2). Presumably, τ_3 represents the effect of concentration gradients across the proteoliposome membrane.

After activation of the Kdp-ATPase, the measured current rises rapidly and decays within a few seconds. This seems to be indicative of a pre-steady-state experiment. However, the conductivity dependence of the signal revealed that the decay is only due to the charging of the proteoliposome membrane. In fact, in the decaying phase of the electrical signal, the enzyme is already in the steady state.

In consequence, under the conditions used in our experiments, the steady state of the pump is reached so rapidly (within approximately 20 ms) that the release of ATP from caged ATP mainly determines the rise of the pump current. This is consistent with a rapid dephosphorylation reaction as proposed previously (Siebers & Altendorf, 1989). The measured peak current therefore yields the properties of the enzyme in the stationary state. No further information about rate constants of partial reactions can be obtained from the electrical signal at the present conditions.

Cation and Anion Dependence of the Kdp-ATPase. The affinity of the Kdp-ATPase to K^+ determined from the electrical experiments is relatively low (50 μM, Figure 8). In the literature, values of $2-10$ μM (Rhoads et al., 1978; Siebers & Altendorf, 1989), depending on the experiment and the experimental conditions, are found. The reason for this discrepancy is unclear. It is unlikely that the accessibility of the K^+ binding site inside the proteoliposomes is responsible for the low affinity determined in the electrical experiments, since addition of K^+ ionophores did not change the results. From the present measurements, we have to conclude that the Kdp-ATPase has an intrinsic K^+ dissociation constant, which is larger than or equal to 50 μM.

At high KCl concentration, a reduction of the signal is observed. It was shown that this is not a specific effect of K^+ acting, e.g., at the K^+ release sites. Other cations which are not transported reduce the signal as well. In addition, the type of anion or cation present matters. This may be indicative of a Hoffmeister effect of chaotropic ions as demonstrated for the Na^+K^+-ATPase (Post & Suzuki, 1991).

Conclusions and a Plausible Transport Model. We have measured the electrogenic transport of the purified Kdp-ATPase reconstituted into liposomes. With a direct current measurement, it was shown that during the Kdp reaction cycle positive charge is transported to the cytoplasmic side of the protein.

The Kdp-ATPase transports K^+ with high affinity. If a transport model analogous to that of the Na^+K^+-ATPase is adopted, the following tentative assignments can be made: The first step after ATP binding is the formation of the phosphointermediates $E_1ATP \rightarrow E_1P \rightarrow E_2P$. This reaction is correlated with either the return of the unloaded K^+ binding sites to the extracellular surface or possibly the transport of one H^+ out of the cell or both (if distinct binding sites for K^+ and H^+ are assumed). This reaction is analogous to Na^+ transport in the Na^+K^+-ATPase. Transport of two K^+ into the cell corresponds to the $E_2 \rightarrow E_1$ transition (as it does in the Na^+K^+-ATPase). Both reactions, K^+ transport and the return of the unloaded K^+ binding sites and/or H^+ transport, can in principle be electrogenic. On the basis of the electrical experiments presented here, we cannot decide which of these partial reactions are electrogenic. Electrical measurements with a higher time resolution are under way to resolve the two transport reactions.

ACKNOWLEDGMENT

We thank Eva Grabsch for excellent technical assistance.

REFERENCES

Altendorf, K., & Epstein, W. (1993) *Cell. Physiol. Biochem. 4*, 160−168.
Altendorf, K., Siebers, A., & Epstein, W. (1992) *Ann. N.Y. Acad. Sci. 671*, 228−243.
Altendorf, K., Voelkner, P., & Puppe, W. (1994) *Res. Microbiol. 145*, 374−381.
Bakker, E. P., & Mangerich, W. E. (1981) *J. Bacteriol. 147*, 820−826.
Bamberg, E., Butt, H.-J., Eisenrauch, A., & Fendler, K. (1991) *Q. Rev. Biophys. 26*, 1−25.
Barabás, K., & Keszthelyi, L. (1984) *Acta Biochim. Biophys. Acad. Sci. Hung. 19*, 305−309.
Borlinghaus, R., Apell, H.-J., & Läuger, P. (1987) *J. Membr. Biol. 97*, 161−178.
Buurman, E. T., Kim, K.-T., & Epstein, W. (1995) *J. Biol. Chem. 270*, 6678−6685.
Cornelius, F. (1988) *Methods Enzymol. 156*, 156−167.
De Weer, P., Gadsby, D. C., & Rakowski, R. F. (1988) *Annu. Rev. Physiol. 50*, 225−241.
Dröse, S., Bindseil, K. U., Bowman, E. J., Siebers, A., Zeeck, A., & Altendorf, K. (1993) *Biochemistry 32*, 3902−3906.
Fendler, K., Grell, E., Haubs, M., & Bamberg, E. (1985) *EMBO J. 4*, 3079−3085.
Fendler, K., Jaruschewski, S., Hobbs, A., Albers, W., & Froehlich, J. P. (1993) *J. Gen. Physiol. 102*, 631−666.
Gadsby, D. C., & Nakao, M. (1989) *J. Gen. Physiol. 94*, 511, 537.
Hilden, S., & Hokin, L. E. (1975) *J. Biol. Chem. 250*, 6296−6303.
Hoffman, J. F., & Laris, P. C. (1974) *J. Physiol. 239*, 519−552.
Kaplan, J. H., Forbush, B., III, & Hoffman, J. F. (1978) *Biochemistry 17*, 1929−1935.
Kollman, R., & Altendorf, K. (1993) *Biochim. Biophys. Acta 1143*, 62−66.
Läuger, P. (1991) in *Electrogenic Ion Pumps*, pp 139−280, Sinauer Associates Inc., Sunderland, MA.

Levy, D., Seigneuret, M., Bluzat, A., & Rigaud, J.-L. (1990) *J. Biol. Chem. 265*, 19524−19534.
Maniatis, T., Fritsch, E. F., & Sambrook, J. (1982) *Molecular Cloning. A laboraty manual*, Cold Spring Harbor Laboratory Press, Cold Spring Harbor, NY.
Nagel, G., Fendler, K., Grell, E., & Bamberg, E. (1987) *Biochim. Biophys. Acta 901*, 239−249.
Post, R. L., & Suzuki, K. (1991) in *The Sodium Pump: Structure, Mechanism and Regulation* (De Weer, P., Kaplan, J., & Forbush, B., Eds.) pp 201−209, The Rockefeller University Press, New York.
Puppe, W., Siebers, A., & Altendorf, K. (1992) *Mol. Microbiol. 6*, 3511−3520.
Rabon, E. C., Mc Fall, T. L., & Sachs, G. (1982) *J. Biol. Chem. 257*, 6296−6299.
Rhoads, D. B., Waters, F. B., & Epstein, W. (1976) *J. Gen. Physiol. 67*, 325−341.
Sachs, G., Chang, H. H., Rabon, E., Schackman, R., Lewin, M., & Saccomani, G. (1976) *J. Biol. Chem. 251*, 7690−7698.
Schaffner, W., & Weissmann, C. (1973) *Anal. Biochem. 56*, 502−514.
Serrano, R. (1988) *Biochim. Biophys. Acta 947*, 1−28.
Siebers, A., & Altendorf, K. (1988) *Eur. J. Biochem. 178*, 131−140.
Siebers, A., & Altendorf, K. (1989) *J. Biol. Chem. 264*, 5831−5838.
Siebers, A., & Altendorf, K. (1992) in *Alkali cation transport systems in procaryotes* (Bakker, E. P., Ed.) pp 225−252, CRC Press, Boca Raton, FL.
Siebers, A., Kollman, R., Dirkes, G., & Altendorf, K. (1992) *J. Biol. Chem. 267*, 12717−12721.
Stengelin, M., Fendler, K., & Bamberg, E. (1993) *J. Membr. Biol. 132*, 211−227.
Walderhaug, M. O., Polarek, J. W., Voelkner, P., Daniel, J. M., Hesse, J. E., Altendorf, K., & Epstein, W. (1992) *J. Bacteriol. 174*, 2152−2159.
Walker, J. W., Reid, G. P., McCray, J. A., & Trentham, D. R. (1988) *J. Am. Chem. Soc. 110*, 7170−7177.

BI960175E